

Global Structure of Forked DNA in Solution Revealed by High-Resolution Single-Molecule FRET

Tara Sabir,^{†,‡} Gunnar F. Schröder,[§] Anita Toulmin,^{†,‡} Peter McGlynn,^{||} and Steven W. Magennis^{*,†,‡}

[†]School of Chemistry, The University of Manchester, Oxford Road, Manchester M13 9PL, U.K.

[‡]The Photon Science Institute, The University of Manchester, Alan Turing Building, Oxford Road, Manchester M13 9PL, U.K.

[§]Institute of Structural Biology and Biophysics, Forschungszentrum Jülich, 52425 Jülich, Germany

^{||}Institute of Medical Sciences, University of Aberdeen, Ashgrove Road West, Aberdeen AB25 2ZD, U.K.

S Supporting Information

ABSTRACT: Branched DNA structures play critical roles in DNA replication, repair, and recombination in addition to being key building blocks for DNA nanotechnology. Here we combine single-molecule multiparameter fluorescence detection and molecular dynamics simulations to give a general approach to global structure determination of branched DNA in solution. We reveal an open, planar structure of a forked DNA molecule with three duplex arms and demonstrate an ion-induced conformational change. This structure will serve as a benchmark for DNA–protein interaction studies.

Branched DNA molecules are central intermediates in genome duplication, where a parental duplex is copied to form two daughter duplexes. They are also central to enzymatic processing of damaged replication forks, repair of DNA damage, and recombination between homologous duplexes.¹ The structures of branched DNA intermediates are therefore likely to impact directly on recognition by a multitude of DNA-processing enzymes. Branched DNA is also widely used as a building block in DNA nanostructures² and nanomechanical devices³ as well as in DNA computation.⁴ Although X-ray crystal structures are available for a small number of such molecules, notably the Holliday junction,⁵ the detailed structures of branched nucleic acids are largely unknown.⁶ We show here that multiparameter fluorescence detection (MFD) of single molecules in combination with molecular dynamics (MD) simulations can reveal the accurate three-dimensional global structure of a three-armed forked DNA molecule in solution.

In view of the potential for static or dynamic heterogeneity in solution,⁷ it is desirable to elucidate the structure of individual branched DNA molecules without ensemble averaging. Atomic force microscopy (AFM) is very effective at probing single molecules in solution and has been successfully used to study DNA nanostructures.⁴ However, distortion of the structure due to interaction with the surface cannot be ruled out, particularly for flexible molecules.⁸ Single-molecule fluorescence resonance energy transfer (SM-FRET), which probes inter- or intramolecular energy transfer between chromophoric labels on the 1–10 nm length scale,⁹ can also be used to study the structure and dynamics of DNA structures that are either immobilized or free

in solution.¹⁰ In spite of this, the use of FRET as a quantitative structural tool is hampered by uncertainties in the positions and orientations of the fluorescent dyes as well as by calibration factors such as detection efficiencies and spectral cross-talk.¹¹ The MFD approach measures the color, lifetime, polarization, and intensity of fluorescence simultaneously¹² and, together with detailed MD simulations of local dye positions, has allowed accurate distance determinations within unbranched double-stranded DNA (dsDNA).¹³

We used MFD of SM-FRET to study a branched DNA molecule, which we term a four-stranded fork (4SF), designed to mimic the possible structure of a blocked replication fork.¹ The DNA sequence of the 4SF and the positions of the fluorescent dyes are shown in Figure 1a. A geometric model of the 4SF is shown in Figure 1b. We considered the branched DNA as three independent helical arms connected by a freely rotating joint, the branch point (see Figure 1b). Orientation of the axis frame of one helical arm with respect to a reference frame of another helical arm requires two polar angles and an angle of rotation around the helical axis; since there are two independent helical axis frames, we required six independent parameters to define the global structure.

We studied fully complementary, immobile branched DNA structures by annealing of single strands that were designed to minimize undesirable base pairing (e.g., hairpin formation) and sequence-specific bending (e.g., A-tracts). For FRET measurements, we investigated branched molecules having a single donor dye, Alexa488, in one of three positions (D1, D2, or D3) and an acceptor dye, Cy5, in one of three positions (A1, A2, or A3). The six dye positions allowed us to measure eight unique distances. We also studied the corresponding donor-only structures to check for local quenching effects.

Previous studies of Holliday junctions have revealed a number of characteristic features of nucleic acid junctions, including their ability to undergo pairwise coaxial stacking and ion-induced folding.⁶ Holliday junctions can undergo both specific and nonspecific interactions with monovalent and multivalent cations, depending on the local ion concentration.⁶ Therefore, we studied the 4SF in two buffers, one containing no Mg²⁺ ions and one with 1 mM MgCl₂ present.

Received: September 24, 2010

Published: December 21, 2010

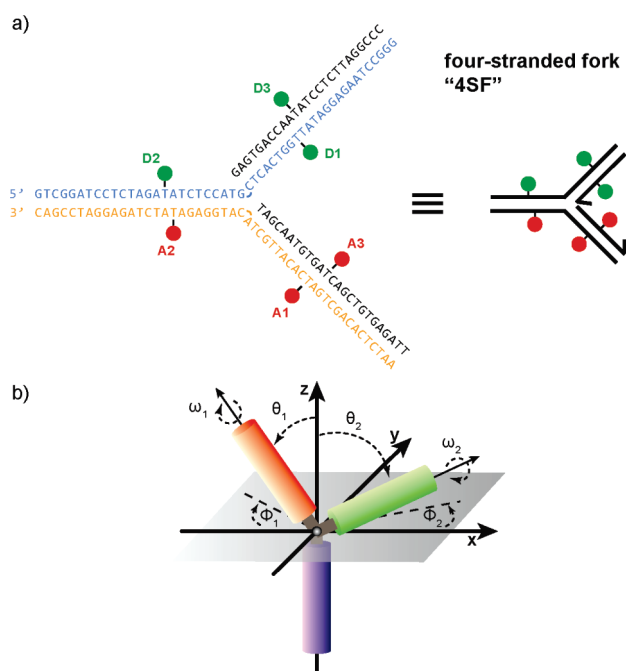


Figure 1. (a) Schematic of the four-stranded fork (4SF) showing the DNA sequence and the positions of the donor (D) and acceptor (A) dyes for single-molecule FRET measurements. A simplified representation is depicted on the right. (b) Geometric model of a 4SF wherein the global structure is defined by the polar angles θ and ϕ and the angle of rotation around the helical axis, ω .

Figure 2 shows typical MFD data for a donor-only control and a donor–acceptor sample. The MFD method uses a confocal microscope with pulsed laser excitation and simultaneous photon-counting detection of fluorescence in four channels (two colors for both parallel and perpendicular polarization).¹² See the Supporting Information for full details of the experimental setup. The two-dimensional (2D) frequency plots are of FRET efficiency (E) or donor anisotropy (r_D) versus donor lifetime ($\tau_{D(A)}$). MFD allows FRET-related species to be unambiguously assigned, since these fall on the theoretical curves highlighted in Figure 2. Photobleaching, dye quenching, and the presence of impurities are easily discerned and do not affect the distance measurement. For every donor-only sample, we observed one main population (Figure 2a). As expected, the Alexa488 had a lifetime of 4.1 ns at all labeling positions. We also observed a minor population with a lifetime of ~ 2 ns, which was observed previously in MFD of Alexa488 and is attributed to a quenched form of the dye.¹⁴ The anisotropy of the donor was low, as observed previously, ruling out dye orientation effects.¹³ For donor–acceptor samples, two populations were observed (Figure 2b); one was identical to that of the donor-only sample (due to unlabeled or photobleached acceptor strand), while the other had a shorter donor lifetime than the donor-only species as well as a reduced donor/acceptor intensity ratio and increased anisotropy. The MFD data demonstrate unambiguously that this second population was due to doubly labeled branched DNA molecules undergoing FRET. The widths of the FRET peaks were similar to those of shot-noise-limited FRET populations measured previously for dsDNA, suggesting either the absence of a static distance distribution or fast dynamics.^{14,15}

To convert these accurate FRET measurements into absolute dye–dye distances, we used a nonlinear conversion function that

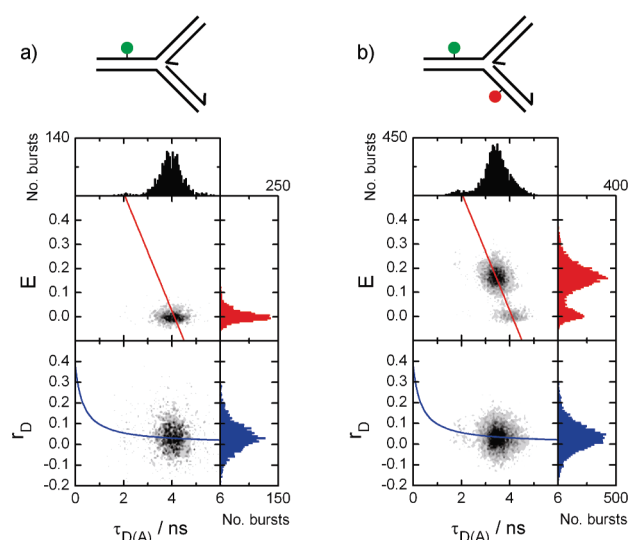


Figure 2. Single-molecule multiparameter fluorescence detection (MFD) of branched DNA. Typical data are shown for a four-stranded fork labeled with (a) a donor dye (at position D2 in Figure 1a) and (b) donor and acceptor dyes (at positions D2 and A1, respectively, in Figure 1a). The 2D plots are of FRET efficiency (E) or donor anisotropy (r_D) versus donor lifetime ($\tau_{D(A)}$). The grayscale indicates an increasing number of single-molecule bursts (from white to black). Also shown are the corresponding 1D histograms. FRET efficiencies were measured from the raw green and red signals and corrected for background (1.54 kHz in green; 2.24 kHz in red), spectral crosstalk (3.5%), detection efficiencies (green/red = 0.3), and the fluorescence quantum yields (0.80 for the donor and 0.32 for the acceptor). The overlaid red line is the theoretical FRET relationship $E = 1 + \tau_D/\tau_{D(A)}$ computed using $\tau_D = 4.1$ ns. The overlaid blue line is the Perrin equation, $r_D = r_0(1 + \tau_{D(A)}/\rho_D)$, in which the mean rotational correlation time (ρ_D) was 0.35 ns and the fundamental anisotropy (r_0) was 0.375. The sample buffer contained 1 mM $MgCl_2$.

Table 1. FRET Distances Calculated from the MFD Data^a

FRET pair	DA distance in 0 mM Mg^{2+} (Å)	DA distance in 1 mM Mg^{2+} (Å) ^b
D1A1	63	66
D1A2	61	62
D1A3	74	69
D2A1	66	69
D2A3	79	80
D3A1	66	65
D3A2	64	64
D3A3	68	68

^a The distances were calculated from the donor lifetimes in the presence of the acceptor by fitting the lifetime histogram of the FRET subpopulation in the MFD plots (e.g., Figure 2b) to a single Gaussian, as described in the Supporting Information. The experiments used a buffer containing 20 mM Tris, 15 mM NaCl, and 1 mM ascorbic acid at pH 7.5. The standard deviation was 2 Å for all of the distances except D1A3 at low $[Mg^{2+}]$, where it was 3 Å. ^b In these experiments, the buffer also contained 1 mM $MgCl_2$.

takes into account the positional and orientational averaging of the dyes (see the Supporting Information).¹³ The calculated distances are given in Table 1.

These dye–dye distances were used as restraints in MD simulations. As the deviations due to sequence-dependent

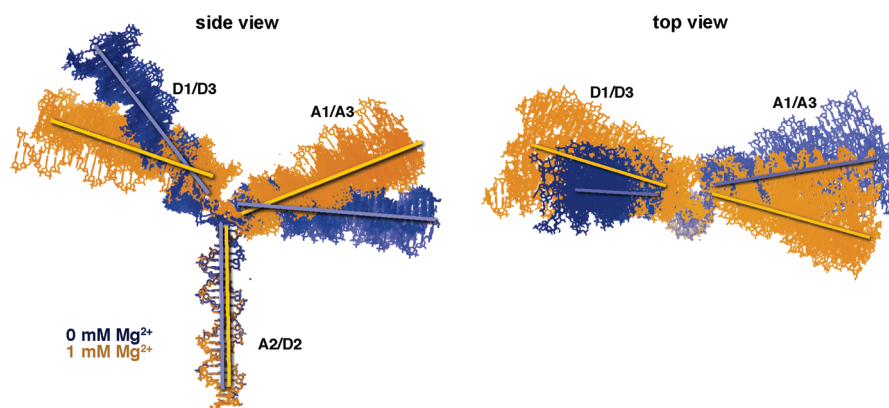


Figure 3. Global structure of the 4SF derived from SM-FRET distance constraints and MD simulations. The five lowest-energy structures are shown for the 4SF in a buffer containing either 0 mM MgCl_2 (blue) or 1 mM MgCl_2 (orange). The average positions of the duplex arms of the helical axes are represented by lines. The angles defining the global structure in 0 mM Mg^{2+} are $\omega_1 = (-47.0 \pm 0.5)^\circ$, $\omega_2 = (6.4 \pm 0.3)^\circ$, $\phi_1 = (-18.1 \pm 0.4)^\circ$, $\phi_2 = (25.6 \pm 0.3)^\circ$, $\theta_1 = (38.8 \pm 0.2)^\circ$, and $\theta_2 = (88.9 \pm 0.2)^\circ$; in 1 mM Mg^{2+} they are $\omega_1 = (-10.9 \pm 0.6)^\circ$, $\omega_2 = (21.3 \pm 2.3)^\circ$, $\phi_1 = (-16.4 \pm 0.9)^\circ$, $\phi_2 = (26.4 \pm 2.6)^\circ$, $\theta_1 = (77.6 \pm 0.3)^\circ$, and $\theta_2 = (66.9 \pm 0.6)^\circ$. See Figure 1b for the definitions of these angles; the subscripts 1 and 2 refer to arms D1/D3 and A1/A3, respectively.

bending are small,¹³ the helical arms of the structures were modeled and restrained as B-DNA. Three different sets of restraints were tested: all base pairs restrained (0-free), one base pair per arm left unrestrained (1-free), and two base pairs per arm unrestrained (2-free). The restraints of the bases included not only base pairing but also base stacking. The distance root-mean-square deviation (DRMSD) between the FRET distances and the dye positions in the model measures how well the model fits the measured FRET distances (Figure S2 in the Supporting Information). As described in the Supporting Information, the 1-free case yielded the lowest DRMSD values while having a small variance (Figures S3–S5). The structures with the five lowest DRMSD values were superimposed and are shown in Figure 3 for solutions containing either 0 mM Mg^{2+} (blue) or 1 mM Mg^{2+} (orange). The structures for a particular sample are very similar to each other, illustrating that we have a well-defined global structure in each case. All of the structures are consistent with full base pairing. The 4SF adopts an open, planar conformation, and there is no evidence of coaxial stacking between any of the helical arms, in contrast to the Holliday junction.⁶

There is a clear difference between the structures in the presence and absence of Mg^{2+} ions. The combination of small but reproducible distance changes results in a significant change in the fitted global structure, with symmetrical twisting around the axis defined by the parent duplex (the A2/D2 arm). There is also an asymmetrical folding whereby the D1/D3 arm is bent toward the parent duplex by $\sim 40^\circ$ while the A1/A3 arm is bent by $\sim 20^\circ$ in the opposite direction.

In summary, we have applied quantitative SM-FRET and MD simulations to determine the global structure of a branched DNA molecule. We have studied the molecule in solution, free from interference from sample heterogeneity and surface effects, and have found that it adopts an open, planar conformation without coaxial stacking of arms. There is evidence for ion-induced folding via interactions with Mg^{2+} ions. The largely symmetrical structure of the 4SF found here in the presence of Mg^{2+} ions may dictate the efficiency of recognition of such structures during processing of damaged replication forks and recombination intermediates. We will explore further the dependence of sequence and local ionic environment on the conformations of these molecules. These structures will serve as the benchmark for our ongoing studies of forked DNA and their interactions with repair enzymes and accessory proteins.

■ ASSOCIATED CONTENT

S Supporting Information. Sample preparation, experimental and computational methods, Figures S1–S5, and PDB files. This material is available free of charge via the Internet at <http://pubs.acs.org>.

■ AUTHOR INFORMATION

Corresponding Author

steven.magennis@manchester.ac.uk

■ ACKNOWLEDGMENT

We thank the BBSRC (BB/G00269X/1) for support and Claus Seidel, Ralf Kühnemuth, Suren Felekyan, Stefan Marawske, Alessandro Valeri, and Evangelos Sisamakakis for assistance in developing our MFD setup. We thank Richard Henchman for helpful discussions. S.W.M. acknowledges the award of an EPSRC Advanced Research Fellowship (EP/D073154).

■ REFERENCES

- (1) (a) Atkinson, J.; McGlynn, P. *Nucleic Acids Res.* **2009**, *37*, 3475–3492. (b) Heller, R. C.; Mariani, K. J. *Nat. Rev. Mol. Cell Biol.* **2006**, *7*, 932–943.
- (2) Aldaye, F. A.; Palmer, A. L.; Sleiman, H. F. *Science* **2008**, *321*, 1795–1799.
- (3) Gu, H. Z.; Chao, J.; Xiao, S. J.; Seeman, N. C. *Nature* **2010**, *465*, 202–205.
- (4) Yin, P.; Choi, H. M. T.; Calvert, C. R.; Pierce, N. A. *Nature* **2008**, *451*, 318–322.
- (5) Ortiz-Lombardía, M.; González, A.; Eritja, R.; Aymami, J.; Azorin, F.; Coll, M. *Nat. Struct. Biol.* **1999**, *6*, 913–917.
- (6) Lilley, D. M. J. *Q. Rev. Biophys.* **2000**, *33*, 109–159.
- (7) (a) Seeman, N. C.; Lukeman, P. S. *Rep. Prog. Phys.* **2005**, *68*, 237–270. (b) Seeman, N. C. In *Algorithmic Bioprocesses*; Condon, A., Harel, D., Kok, J. N., Salomaa, A., Winfree, E., Eds.; Springer-Verlag: Berlin, 2009; pp 205–214.
- (8) Lyubchenko, Y. L.; Shlyakhtenko, L. S. *Methods* **2009**, *47*, 206–213.
- (9) (a) Weiss, S. *Science* **1999**, *283*, 1676–1683. (b) Roy, R.; Hohng, S.; Ha, T. *Nat. Methods* **2008**, *5*, 507–516.
- (10) (a) McKinney, S. A.; Déclais, A.-C.; Lilley, D. M. J.; Ha, T. *Nat. Struct. Biol.* **2003**, *10*, 93–97. (b) Joo, C.; McKinney, S. A.; Lilley,

D. M. J.; Ha, T. *J. Mol. Biol.* **2004**, *341*, 739–751. (c) Person, B.; Stein, I. H.; Steinhauer, C.; Vogelsang, J.; Tinnefeld, P. *ChemPhysChem* **2009**, *10*, 1455–1460. (d) Ying, L. M.; Green, J. J.; Li, H. T.; Klenerman, D.; Balasubramanian, S. *Proc. Natl. Acad. Sci. U.S.A.* **2003**, *100*, 14629–14634.

(11) Clegg, R. M. *Methods Enzymol.* **1992**, *211*, 353–388.

(12) (a) Rothwell, P. J.; Berger, S.; Kensch, O.; Felekyan, S.; Antonik, M.; Wöhrle, B. M.; Restle, T.; Goody, R. S.; Seidel, C. A. M. *Proc. Natl. Acad. Sci. U.S.A.* **2003**, *100*, 1655–1660. (b) Gansen, A.; Valeri, A.; Hauger, F.; Felekyan, S.; Kalinin, S.; Tóth, K.; Langowski, J.; Seidel, C. A. M. *Proc. Natl. Acad. Sci. U.S.A.* **2009**, *106*, 15308–15313.

(13) Woźniak, A. K.; Schröder, G. F.; Grubmüller, H.; Seidel, C. A. M.; Oesterhelt, F. *Proc. Natl. Acad. Sci. U.S.A.* **2008**, *105*, 18337–18342.

(14) Kalinin, S.; Sisamakis, E.; Magennis, S. W.; Felekyan, S.; Seidel, C. A. M. *J. Phys. Chem. B* **2010**, *114*, 6197–6206.

(15) Mathew-Fenn, R. S.; Das, R.; Harbury, P. A. B. *Science* **2008**, *322*, 446–449.

■ NOTE ADDED AFTER ASAP PUBLICATION

Table 1, footnote *a*, was corrected January 11, 2011.